Nature of the Species Present in the Zirconocene Dichloride−Butyllithium Reaction Mixture

Vladimir K. Dioumaev and John F. Harrod*

Chemistry Department, McGill University, Montreal, Quebec, Canada H3A 2K6

Received July 3, 1996[⊗]

The thermal decomposition of dibutylzirconocene (**1**) at room temperature affords paramagnetic butylzirconocene(III) (**11**), zirconocene(III) hydride (**12**), the diamagnetic butenylzirconocene(IV) hydride dimer **5a**, and the 1,1-bis(cyclopentadienyl)-2-methyl-3-(zirconocenyl hydride)-1-zirconacyclobutane(IV) dimer **9**. Initially, decomposition furnishes crotylzirconocene(IV) hydride (**3a**), followed by 1,1-bis(cyclopentadienyl)-2-ethyl-1-zirconacyclopropane(IV) (**2a**) and 1,1-bis(cyclopentadienyl)-3,4-diethyl-1-zirconacyclopentane(IV) (**4a**), listed in the order of appearance. This order suggests that the primary decomposition reaction is a γ-H abstraction, which leads to the formation of 1,1-bis(cyclopentadienyl)-2-methyl-1-zirconacyclobutane(IV) (**6a**). The latter was not observed experimentally but is postulated on the basis of secondary products. Reactions leading to the above compounds are discussed from mechanistic and thermochemical points of view. The reported compounds have been characterized by either EPR or multidimensional, multinuclear NMR spectroscopy. Compound **3a** has also been synthesized independently from zirconocene chloride hydride and crotylmagnesium bromide and undergoes the same rearrangements into **2a** and then **4a**. The allyl analog **3b**, synthesized from zirconocene chloride hydride and allylmagnesium bromide, exhibits the same behavior and rearranges into 1,1-bis(cyclopentadienyl)-3,4-dimethyl-1-zirconacyclopentane (**4b**).

Introduction

Cp_2ZrCl_2/2RLi (R = alkyl) reagents have found widespread use in organic synthesis and in catalysis.[1] Despite a long history of study of the chemistry of such systems, the exact nature of the reactive species in solution, at room temperature, remains unclear. The primary reaction is simple and leads to the formation of the dialkylzirconocene **1** (eq 1), which in most cases is thermally unstable but can be characterized in solution at low temperatures by spectroscopic methods.[1]

$$Cp_2ZrCl_2 + 2\ n\text{-BuLi} \longrightarrow \underset{\mathbf{1}}{Cp_2Zr(n\text{-Bu})_2} + 2LiCl \qquad (1)$$

The thermal decomposition reactions of the dialkylzirconocenes are more poorly documented, but it is clear that a number of ill-characterized compounds are formed. Only three reliable conclusions can be drawn from the numerous experiments described in the literature.[2−8] First, the main gaseous product is the corresponding alkane RH, as observed by mass spectroscopy and GC.[2,8] Continuous heating of the reaction mixture above room temperature, or reaction with alkenes, produces the alkene R(−H).[7,8] Second, phosphine adducts of alkenezirconocene complexes, $Cp_2Zr(RCH{=}CH_2)(PR'_3)$ (R = H, Me, Et, Ph, PR'_3 = PMe_3; R = H, Et, PR'_3 = $PPhMe_2$, PPh_2Me), can be trapped, isolated from the reaction mixture, and fully characterized.[3,4] Third, the structural characterization of a phosphine-free titanocene complex, $Cp^*_2Ti(CH_2{=}CH_2)$, lends support to the possible existence of zirconocene−alkene complexes, albeit analogous compounds of higher olefins could not be isolated.[5]

It may thus be concluded with some confidence that the dialkylzirconocenes undergo hydrogen abstraction, with liberation of alkane and formation of the zirconocene−alkene complex **2** (eq 2). However, the formation of **2** in the absence of phosphine is not unequivocal. Thermally stable titanacyclopentanes, for example, are known to decompose in the presence of phosphines and to form $[Ti](CH_2{=}CH_2)(PMe_3)$.[6] To date, **2** has been neither isolated nor characterized spectroscopically. There have been reports of resonances in the Cp region

$$Cp_2Zr(CH_2CH_2R)_2 \longrightarrow \underset{-\ HCH_2CH_2R}{} \qquad (2)$$

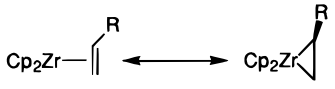

2a R=Et
2b R=Me

* To whom correspondence should be addressed. E-mail: Harrod@omc.lan.McGill.ca.

[⊗] Abstract published in *Advance ACS Abstracts,* February 15, 1997.

(1) Negishi, E.; Takahashi, T. *Acc. Chem. Res.* **1994**, *27*, 124−130 and references cited therein.
(2) Lewis, D. P.; Whitby, R. J.; Jones, R. V. H. *Tetrahedron* **1995**, *51*, 4541−4550.
(3) Takahashi, T.; Murakami, M.; Kunishige, M.; Saburi, M.; Uchida, Y.; Kozawa, K.; Uchida, T.; Swanson, D. R.; Negishi, E. *Chem. Lett.* **1989**, 761−764.
(4) Binger, P.; Muller, P.; Benn, R.; Rufinska, A.; Gabor, B.; Kruger, C.; Betz, P. *Chem. Ber.* **1989**, *122*, 1035−1042.
(5) Cohen, S. A.; Auburn, P. R.; Bercaw, J. E. *J. Am. Chem. Soc.* **1983**, *105*, 1136−1143.
(6) Hill, J. E.; Fanwick, P. E.; Rothwell, I. P. *Organometallics* **1992**, *11*, 1771−1773.
(7) Chang, B.-H.; Tung, H.-S.; Brubaker, C. H. J. *Inorg. Chim. Acta* **1981**, *51*, 143−148.
(8) Kesti, M. R.; Waymouth, R. M. *Organometallics* **1992**, *11*, 1095−1103.

S0276-7333(96)00543-2 CCC: $14.00

of the NMR spectra, which can be due to **2** or any other intermediate, but no detailed investigation has been described.[9−12]

Research in this area has primarily been focused on organic products of the Negishi reaction, and the fate of zirconocene products, apart from mentioning hypothetical **2**, is usually neglected. In the course of our investigations of silane dehydrocoupling catalysts derived from Cp_2ZrCl_2/2BuLi/$B(C_6F_5)_3$,[13−15] a number of questions arose which encouraged us to study the chemistry of the Cp_2ZrCl_2/2BuLi system in greater detail. The results of this study are reported herein.

Results

A mixture of Cp_2ZrCl_2 and BuLi in toluene or THF at −40 °C gave a quantitative conversion to a single product, Cp_2ZrBu_2, identified by its ^{1}H and ^{13}C NMR spectra (Table 1). Assignments of the ^{1}H and ^{13}C resonances were confirmed by ^{1}H COSY and ^{1}H−^{13}C HMQC experiments. The NMR spectra for the new product were distinctly different from the ones for the starting BuLi.[16,17]

A cold solution of Cp_2ZrBu_2 (−40 °C) was warmed slowly to 20 °C until spectral evidence for thermal decomposition was apparent. It was then cooled down (0 through −40 °C) to prevent further decomposition. To obtain a larger and more convincing data set, three independent samples for each solvent (toluene and THF) were studied at slightly different temperatures and different warmup times. Each of the samples was subjected to a number of decomposition−freeze−measurement cycles, and a set of TOCSY, HMQC, COSY, and NOESY experiments were performed. In every case a number of compounds were formed. COSY and TOCSY experiments were particularly useful for the identification of the resonances belonging to the same ligand, as both techniques reveal *J*-coupled protons. TOCSY unambiguously separated ^{1}H NMR signals in groups belonging to different ligands, whereas COSY established a chainwise connectivity of the backbone within a ligand. When the *J* coupling was too weak to show a cross peak, or when the cross peaks were severely overlapped, the evolution of peak intensities with time gave additional information. ^{1}H−^{13}C HMQC data were extremely important to differentiate between allyl, alkenyl, and alkyl ligands, as well as to identify methylene groups with magnetically inequivalent protons. When a heavy overlap of signals precluded direct determination of multiplicity and line shape, this information was retrieved in a 1D TOCSY experiment, although accurate coupling constants cannot be extracted this way. Finally, NOESY helped determine a 3D structure and ligand conformations as well as put together structural fragments, which do not exhibit any *J* coupling (such as Cp, hydride, and hydrocarbyl ligands belonging to the same Zr center). Decomposition pathways proved to be the same for toluene and THF solutions. The latter has been scrutinized more thoroughly because of a wider use of THF with the Cp_2ZrCl_2/2BuLi system.

Despite considerable overlap of NMR resonances in the aliphatic region, a number of compounds can be identified. Thus, a characteristic set (−CH_2CH=CHCH_3) of *J*-coupled (COSY) cross peaks in the ^{1}H NMR spectrum (Table 1) with the corresponding set of ^{13}C resonances, extracted from a ^{1}H−^{13}C HMQC experiment, clearly indicates a crotylzirconocene fragment.[18−24] Under certain conditions (the first 10−30 min at room temperature in toluene or the first 10 min at room temperature in THF) crotylzirconocene hydride (**3a**) was the main observable metallocene compound in the mixture, apart from the unreacted Cp_2ZrBu_2, as judged by the number of peaks in the Cp regions of the ^{1}H and ^{13}C spectra (Figure 1). The other ligand in this compound, a hydride, can be observed in TOCSY and NOESY experiments. The analogous compound Cp^*_2-Zr(CH_2CH=CHCH_3)H, albeit poorly characterized, has been synthesized before by the thermal rearrangement of Cp^*_2Zr(C(Me)=CH(Me))H.[25]

The observation of allylic products is not entirely unexpected, since the decomposition of alkyl- to allylmetallocenes has been previously raised as a possibility in the context of Ziegler−Natta olefin polymerization catalysis.[20,26] Formation of a zirconocene(IV) hydride is of interest, as we believe it to be a key step in the redox reactions occurring in the Cp_2ZrBu_2 system (*vide infra*).

It should be noted that the Cp, C_aH_2, and C_cH proton resonances of **3a** are very broad, while the Me line is only slightly broadened and the C_bH signal is sharp (Figure 1). This broadening stems from a dynamic process, which strongly suggests $\pi-\sigma-\pi$ rearrangement with rotation about the C_a-C_b and C_a−Zr bonds (Figure 2).[27,28] The pairs of diastereotopic Cp and C_aH_2 signals are in exchange and give rise to negative NOE cross peaks. This indicates rotation about the C_a-C_b bond. Such a rotation furnishes two enantiomers, **3′a** and **3″a** (Figure 2), which have inverted labels of the diastereotopic Cp rings and crotyl C_aH_2 protons. This process is slow on the NMR time scale, and the pairs of dynamically equivalent resonances still appear as sepa-

(9) Negishi, E.; Cederbaum, F. E.; Takahashi, T. *Tetrahedron Lett.* **1986**, *27*, 2829−2832.
(10) Negishi, E.; Holmes, S. J.; Tour, J. M.; Miller, J. A.; Cederbaum, F. E.; Swanson, D. R.; Takahashi, T. *J. Am. Chem. Soc.* **1989**, *111*, 3336−3346.
(11) Hoveyda, A. H.; Morken, J. P. *J. Org. Chem.* **1993**, *58*, 4237−4244.
(12) Didiuk, M. T.; Johannes, C. W.; Morken, J. P.; Hoveyda, A. H. *J. Am. Chem. Soc.* **1995**, *117*, 7097−7104.
(13) Dioumaev, V. K.; Harrod, J. F. *Organometallics* **1994**, *13*, 1548−1550.
(14) Dioumaev, V. K.; Harrod, J. F. *J. Organomet. Chem.* **1996**, *521*, 133−143.
(15) Dioumaev, V. K.; Harrod, J. F. *Organometallics* **1996**, *15*, 3859−3867.
(16) Bauer, W.; Clark, T.; Schleyer, P. v. R. *J. Am. Chem. Soc.* **1987**, *109*, 970−977.
(17) Bauer, W.; Schleyer, P. v. R. *J. Am. Chem. Soc.* **1989**, *111*, 7191−7198.
(18) Tjaden, E. B.; Casty, G. L.; Stryker, J. M. *J. Am. Chem. Soc.* **1993**, *115*, 9814−9815.
(19) Tjaden, E. B.; Stryker, J. M. *J. Am. Chem. Soc.* **1993**, *115*, 2083−2085.
(20) Jeske, G.; Lauke, H.; Mauermann, H.; Swepston, P. N.; Schumann, H.; Marks, T. J. *J. Am. Chem. Soc.* **1985**, *107*, 8091−8103.
(21) Hanzawa, Y.; Harada, S.; Nishio, R.; Taguchi, T. *Tetrahedron Lett.* **1994**, *35*, 9421−9424.
(22) Dimmock, P. W.; Whitby, R. J. *J. Chem. Soc., Chem. Commun.* **1994**, 2323−2324.
(23) Balaich, G. J.; Hill, J. E.; Waratuke, S. A.; Fanwick, P. E.; Rothwell, I. P. *Organometallics* **1995**, *14*, 656−665.
(24) Gordon, G. J.; Whitby, R. J. *Synlett* **1995**, 77−78.
(25) McDade, C.; Bercaw, J. E. *J. Organomet. Chem.* **1985**, *279*, 281−315.
(26) Dorf, U.; Engel, K.; Erker, G. *Angew. Chem., Int. Ed. Engl.* **1982**, *21*, 914−915.
(27) Vrieze, K. In *Dynamic Nuclear Magnetic Resonance Spectroscopy*; Jackman, L. M., Cotton, F. A., Ed.; Academic: New York, 1975; p 441.
(28) Trost, B.; Vranken, D. L. V. *Chem. Rev.* **1996**, *96*, 395−422.

Table 1. NMR Data

compd, solvent, temp (°C)	assignt	^{1}H: δ (ppm), multiplicity (coupling const, Hz)[a]	^{13}C: δ (ppm)
1, toluene-d_8, −20	α-Bu	0.31, m	53.9
	β-Bu	1.41, m	35.5
	γ-Bu	1.34, m	30.4
	δ-Bu	1.04, t (6.8)	14.5
	Cp(#1 and 2)	5.6, s	110.3
1, THF-d_8, −20	α-Bu	0.23, m	53.7
	β-Bu	1.35, quintet (8.0)	35.7
	γ-Bu	1.06, sextet (7.2)	30.5
	δ-Bu	0.79, t (7.3)	14.2
	Cp(#1 and 2)	6.06, s	111.2
2a, THF-d_8, −20	Zr*CH*$_2$CHCH$_2$Me	0.02, dd (6.6, 10.0)	34.9
		0.68, t (6.6)	34.9
	ZrCH$_2$*CH*CH$_2$Me	1.33, m	57.6
	ZrCH$_2$CH*CH*$_2$Me	1.42, m	35.0
		1.66, m	35.0
	ZrCH$_2$CHCH$_2$*Me*	0.96, t (7.1)	20.8
	Cp(#1)	5.50, s	105.2
	Cp(#2)	5.52, s	104.8
3a, toluene-d_8, −10	Zr*CH*$_2$CH=CHMe	0.78, br s	35.4
		2.35, br s	35.4
	ZrCH$_2$*CH*=CHMe	3.82, ddd (10.8, 11.2, 15.8)	114.3
	ZrCH$_2$CH=C*H*Me	2.75, br s	80.9
	ZrCH$_2$CH=CH*Me*	2.12, br d (5.6)	21.7
	ZrH	n.d.	na
	Cp(#1)	5.03, br s	98.8
	Cp(#2)	5.19, br s	100.8
3a, THF-d_8, −20	Zr*CH*$_2$CH=CHMe	0.85, br s	35.8
		2.36, br s	35.8
	ZrCH$_2$*CH*=CHMe	4.06, ddd (9.3, 13.7, 15.2)	114.7
	ZrCH$_2$CH=C*H*Me	2.84, br s	80.9
	ZrCH$_2$CH=CH*Me*	2.03, br d (5.7)	21.6
	ZrH	1.09, br s	na
	Cp(#1)	5.31, br s	99.5
	Cp(#2)	5.48, br s	101.4
4a, toluene-d_8, 25	Zr*CH*$_2$CHCH$_2$Me	0.41, dd (4.4, 12.2)	46.2
		1.29, t (12.2)	46.2
	ZrCH$_2$*CH*CH$_2$Me	1.60, m	47.5
	ZrCH$_2$CH*CH*$_2$Me	1.00, m	30.8
		1.62, m	30.8
	ZrCH$_2$CHCH$_2$*Me*	0.94, t (7.1)	10.8
	Cp(#1 and 2)	5.84, s	111.5
4a, THF-d_8, −20	Zr*CH*$_2$CHCH$_2$Me	0.29, dd (4.0, 12.0)	45.5
		1.18, t (12.0)	45.5
	ZrCH$_2$*CH*CH$_2$Me	1.48, m	47.5
	ZrCH$_2$CH*CH*$_2$Me	0.72, m	30.6
		1.29, m	30.6
	ZrCH$_2$CHCH$_2$*Me*	0.68, t (7.0)	10.5
	Cp(#1 and 2)	6.29, s	112.2
4b, THF-d_8, −40	Zr*CH*$_2$CHMe	0.26, dd (3.5, 12.2)	51.1
		1.28, t (12.2)	51.1
	ZrCH$_2$*CH*Me	1.45, m	44.2
	ZrCH$_2$CH*Me*	0.58, d (5.4)	27.1
	Cp(#1 and 2)	6.28, s	112.3
5a, THF-d_8, −40	Zr*CH*=CHCH$_2$Me	8.44, d (17.9)	210.5
	ZrCH=C*H*CH$_2$Me	4.18, ddd (5.9, 7.0, 17.9)	99.8
	ZrCH=CH*CH*$_2$Me	0.98, m	36.2
		1.90, m	36.2
	ZrCH=CHCH$_2$*Me*	0.52, t (6.8)	17.4
	ZrH	-7.80	na
	Cp(#1)	5.92	104.6
	Cp(#2)	5.94	106.2
9, toluene-d_8, −10	Zr*CH*$_2$CHCHMe	0.42, dd (7.7, 12.2)	59.3
		3.06, dd (7.7 and 10.9)	59.3
	ZrCH$_2$*CH*CHMe	−0.69, ddd (10.9, 12.2, 14.0)	40.6
	ZrCH$_2$CH*CH*Me	0.68, m	77.2
	ZrCH$_2$CHCH*Me*	2.04, d (6.7)	31.3
	ZrH	−6.66, s	na
	Cp(#1)	5.30, s	104
	Cp(#2)	5.325, s	104
	Cp(#3)	5.33, s	104
	Cp(#4)	5.34, s	104
9, THF-d_8, 25	Zr*CH*$_2$CHCHMe	0.34, dd (7.6, 12.6)	59.4
		2.93, dd (7.6, 10.9)	59.4
	ZrCH$_2$*CH*CHMe	−0.61, ddd (10.9, 12.6, 14.2)	40.8
	ZrCH$_2$CH*CH*Me	0.66, m	77.6
	ZrCH$_2$CHCH*Me*	1.79, d (6.6)	30.7
	ZrH	−6.55, s	na
	Cp(#1)	5.56, s	104.5
	Cp(#2 and 3)	5.58, s	104.5
	Cp(#4)	5.60, s	105.0

[a] The coupling constants for most of the resonances are not reported, as the signals are either second-order multiplets or are too broad for an accurate value to be determined. Abbreviations: s, singlet; t, triplet; m, multiplet; br s, broad singlet; nd, not determined; na, not applicable.

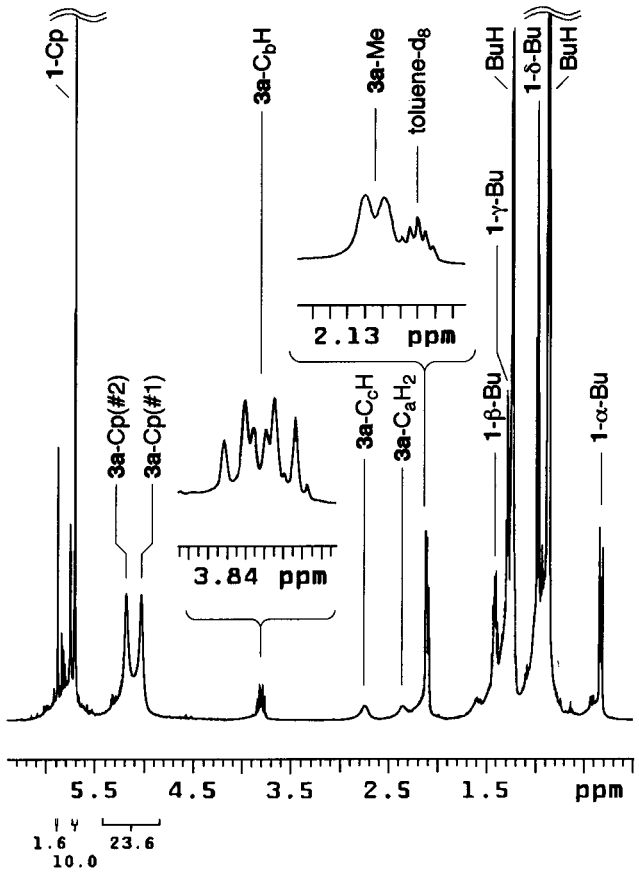

Figure 1. ^{1}H NMR spectrum of a mixture of **1** and **3a** in toluene-d_8 at +25 °C. The Cp, C_aH_2, C_cH, and Me signals of **3** exhibit dynamic broadening, while C_bH is sharp.

rate peaks. The other crotyl resonances should be little affected by this process, as they are enantiotopic in the two rotamers; hence, their magnetic environment does not change. On the other hand, a $\pi-\sigma-\pi$ rearrangement with rotation about the C_a-Zr bond does change local anisotropy for all proton nuclei, as it generates diastereomers (e.g. **3″a** and **3‴a**). This would lead to a doubling of all resonances, or a single set of broad peaks, when rotation is fast on the NMR time scale. However, it would not lead to an exchange between the pairs of Cp and C_aH_2 resonances. The relatively narrow linewidth for the Me resonance indicates that this group is influenced by the anisotropic zirconocene core to a much smaller extent due to its remote position. The only proton which is obviously not affected by this process is C_bH as it is in essentially identical magnetic environments in both rotamers. The signals for C_bH in rotamers **3″a** and **3‴a** coincide and do not cause any broadening. The observed resonance is in fact sharp and exhibits well-resolved scalar coupling to the rest of the crotyl ligand. The coupling is not averaged by dynamic exchange, as one of the processes is slow on the NMR time scale (rotation about the C_a-C_b bond) and the other does not change the spatial relationship of the proton nuclei within the crotyl ligand (rotation about the C_a-Zr bond). Experimentally observed line shapes and NOE cross peaks thus confirm the $\pi-\sigma-\pi$ rearrangement with a slow, yet observable, rotation about the C_a-C_b bond and a fast one about the C_a-Zr bond.

The second product formed in the Cp_2ZrCl_2/2BuLi system is **2a** (Table 1), which appears almost simultaneously with **3a** and is derived from it. When **3a** was

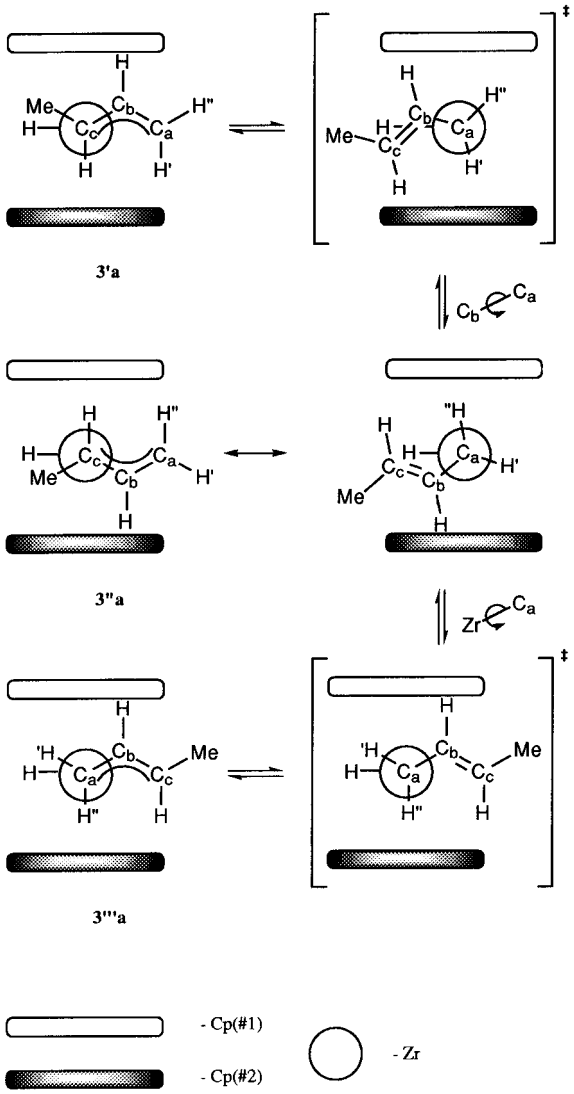

Figure 2. Schematic representation of the $\pi-\sigma-\pi$ dynamic processes in **3a**.

synthesized independently (eq 3), it slowly rearranged

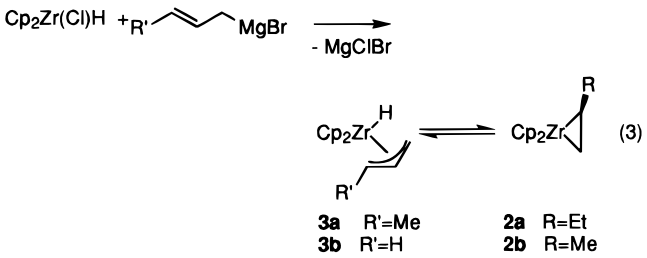

into **2a** even at −40 °C. The latter compound can be readily assigned by a combination of COSY and HMQC experiments, which reveal a $-CH_2CHCH_2CH_3$ backbone with two diastereotopic CH_2 groups (Figure 3) separated by a CH spacer. This assignment is also supported by TOCSY and NOESY spectra, by integrals, and by simultaneous buildup (or decay) of all $CH_2CHCH_2CH_3$ signals with time. The multiplicity of the C_aH_2 group (Figure 4) is characteristic of a small cycle with two diastereotopic geminal protons having considerably different coupling constants (gauche and eclipsed) to the same vicinal neighbor. The large difference in the values is typical for rigid rings with little conformational freedom, where the torsion angles are not averaged by free rotation. The ^{1}H and ^{13}C NMR spectra of **2a** are

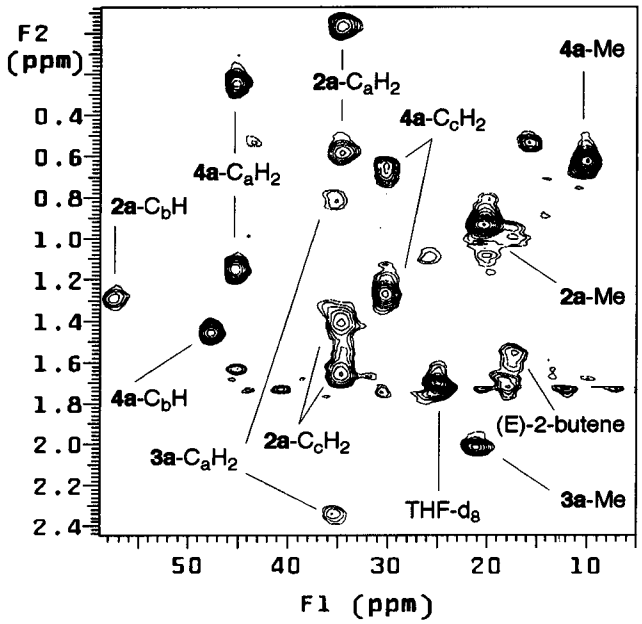

Figure 3. $^1H-^{13}C$ HMQC spectrum of a mixture of **2a**, **3a**, and **4a** in THF-d_8 at −40 °C. Pairs of cross peaks having a common ^{13}C chemical shift belong to diastereotopic methylene groups.

similar to those of the well-characterized phosphine adduct $Cp_2Zr(EtCH{=}CH_2)(PMe_3)$.[3,4] To the best of our knowledge, this is the first characterization of this long-postulated intermediate.

Compounds **2a** and **3a** are in an equilibrium which is significantly shifted toward **2a**, which proves that **2a** cannot be a primary product in the decomposition of **1**. Indeed, if **2a** were formed prior to **3a**, the concentration of the latter would never exceed the concentration of the former. The equilibrium can be observed by NOESY at 0 °C. Thus, in addition to the negative NOE cross peaks, due to the dynamic exchange in the fluxional crotyl complex (*vide supra*), there is another set of negative cross peaks between certain pairs of protons in **2a** and **3a** (Figure 5). Dynamic exchange of both C_aH_2 resonances of **3a** with every C_aH_2 signal of **2a** (Figures 5 and 6) indicates that the process, which scrambles C_aH_2 in **3a** and converts rotamer **3′a** into **3″a** and then into **2″a** (or **3″a** → **3′a** → **2′a**), is sufficiently fast on the NMR time scale to be observed. On the other hand, **2′a** and **2″a** are enantiomers, which have inverted labels of C_aH' and C_aH'' protons. There is, however, no scrambling of the C_aH_2 resonances of **2a**, which means that neither **2′a** → **3′a** → **3″a** → **2″a** nor **2″a** → **3″a** → **3′a** → **2′a** is fast enough to be observable under the same conditions. It should be noted that the hydrogen addition−elimination, which interconverts **2a** and **3a**, is face-selective and scrambles proton labels exclusively within C_cH-**2a**/C_cH-**3a** and C_cH*-**2a**/ZrH*-**3a** pairs. The lack of C_cH-**2a**/ZrH*-**3a** and C_cH*-**2a**/C_cH-**3a** cross-scrambling indicates that the β-H elimination, **2a** → **3a**, occurs more readily from the C_cH* position. This can be explained in terms of steric repulsion between Me and Cp groups, with one rotamer of **2a**, where the Me group points away from both Cp ligands, being significantly lower in energy. The H*−C_c bond in this rotamer lies almost in the bisectorial plane, as required for the elimination to occur.

The observation of such an exchange lends additional support for the assignment of structures **2a** and **3a**, as it interlocks similar positions in the skeletons of the two molecules. It also reveals an important feature of the Cp_2ZrBu_2 reagent: there are a number of species present in it, but they are in equilibrium with each other, and if only one compound is consumed in a given reaction, the whole system can evolve toward it. This explains the versatile behavior of the Cp_2ZrBu_2 reagent in various constant- and variable-oxidation-state reactions, as different reactions can be driven by different species present in that system, even if their concentration is not high.

Longer decomposition times (several hours at −20 or −40 °C or minutes at room temperature) lead to the disappearance of **2a** and **3a** and formation of **4a**. A bis(pentamethylcyclopentadienyl) (Cp*) analog of the latter has been previously described by Bercaw *et. al.*[25] and further characterized by Marks *et. al.*[29] The connectivity pattern in **4a**, readily obtained from a combination of TOCSY, COSY, and HMQC experiments, is very similar to **2a** (Figures 3 and 4). Indeed, the hydrocarbyl skeleton of the former (−CH_2(Et)CHCH(Et)CH_2−) can be viewed as a dimer of the latter. The halves of the dimer are related by a C_2 symmetry operation; thus, only one set of NMR peaks is observed. The zirconacyclopentane **4a**, however, has two features, distinctly different from **2a**: the Cp groups, assigned by NOESY, are equivalent (related by C_2 symmetry) and integration of Cp versus −$CH_2CHCH_2CH_3$ gives two hydrocarbyls per sandwich. Further, the ^1H and ^{13}C chemical shifts are almost identical with the ones described for the previously prepared Cp* analog.[25,29]

Further thermal decomposition leads to the disappearance of **4a** and accumulation of **5a** and **9**. The former is produced in minor quantities but can be readily identified by the characteristic signals of its vinylic group (^1H, 8.44 ppm, d and 4.18 ppm, ddd; ^{13}C, 210.5 and 99.8 ppm, respectively), its −CH=$CHCH_2$-Me backbone (identified by COSY and TOCSY), and its strongly shielded μ-H at −7.80 ppm (identified by TOCSY and NOESY). The CH_2 group in **5a** is diastereotopic, reflecting a lack of a mirror plane, which usually coincides with the bisectorial plane in such complexes. Such a reduction of symmetry implies that the vinyl ligand is spatially constrained in some fashion, but none of the experimental data give any indication of what the nature of this constraint is. The other compound, **9**, starts to form at the early stages of decomposition (after the first 20 min at room temperature) and persists for weeks at room temperature. A TOCSY spectrum shows that one of the ligands in this compound exhibits five well-resolved multiplets, which are assigned by COSY and HMQC experiments to a linear $CH_2CHCHCH_3$ fragment with saturated C−C bonds. If this is not a carbocycle and has no multiple C−C bonds, it has to have three C−Zr bonds. Indeed, the NOESY spectrum proves that this ligand is in close proximity to four Cp groups (two zirconocene fragments). It also shows that the other ligand is a hydride and the two zirconocenes are bonded to the (α,γ) and β positions of the carbon chain. Figure 7a schematically represents a fragment of the 3D structure of **9**, which is based on the previously reported geometry of titanacyclobutanes[30] and which explains the observed NOE

(29) Schock, L. E.; Marks, T. J. *J. Am. Chem. Soc.* **1988**, *110*, 7701−7715.

(30) Lee, J. B.; Gajda, G. J.; Schaefer, W. P.; Howard, T. R.; Ikariya, T.; Straus, D. A.; Grubbs, R. H. *J. Am. Chem. Soc.* **1981**, *103*, 7358−7361.

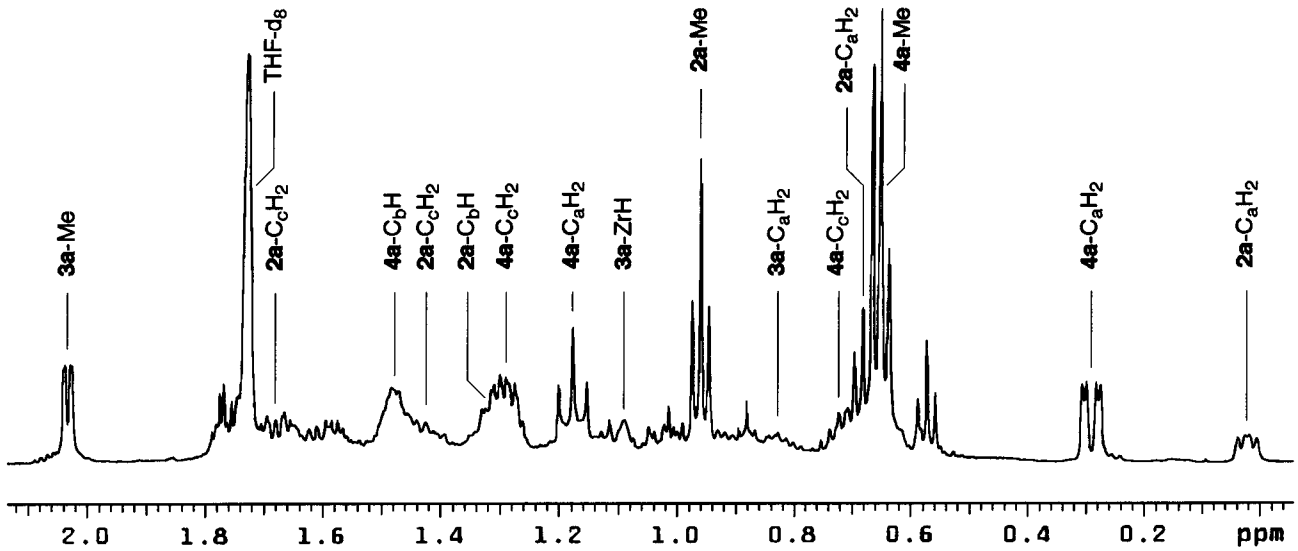

Figure 4. ^{1}H NMR spectrum of a mixture of **2a**, **3a**, and **4a** in THF-d_8 at −20 °C. The multiplicity of the C_aH_2 group in **2a** and **4a** is characteristic of a small cycle with two diastereotopic geminal protons having considerably different coupling constants, gauche and eclipsed, to the same vicinal neighbor.

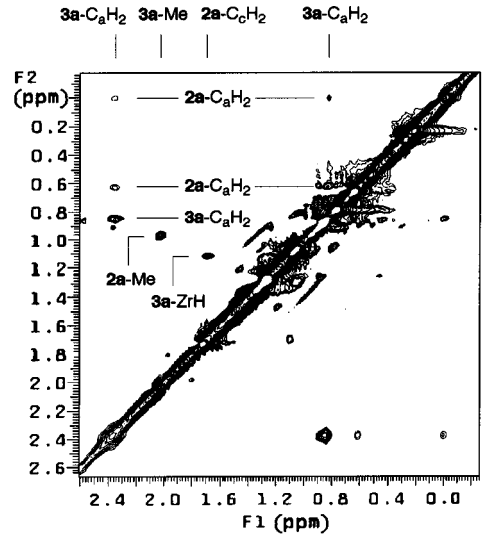

Figure 5. ^{1}H−^{1}H NOESY spectrum (negative contours) of a mixture of **2a** and **3a** in THF-d_8 at 0 °C. Both C_aH_2 resonances of **3a** are in dynamic exchange with each other and with every C_aH_2 signal of **2a**. However, there is no exchange within C_aH_2 and C_cH_2 pairs of **2a**.

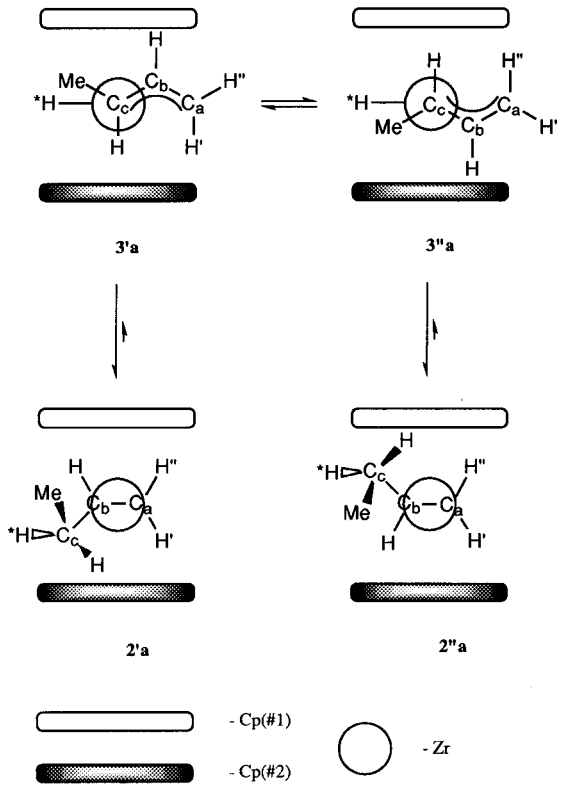

Figure 6. Schematic representation of a dynamic exchange between **2a** and **3a**.

cross peaks. The steric bulk of the zirconacyclobutane ligand constrains the spatial arrangement of the zirconocene fragments so that their bisectorial planes form a close to zero dihedral angle. That way the zirconacycle lies as close as possible to the bisectorial planes of both zirconocenes. The zirconacyclobutane faces the Cp_2Zr_b wedge with its unsubstituted side so that the Me substituent is in a trans arrangement with Zr_b to minimize steric repulsion. As can be seen from Figure 7a, and can be confirmed by simple geometrical estimations, there is only one proton in close proximity to an H−Zr bond. Indeed, the only strong NOE cross peak between hydride and alkyl ligands is between H−Zr and H_b.

The ^{13}C chemical shifts in **9** indicate the same type of structure. Thus, C_β is in a field too strong for a C nucleus directly bonded to zirconocene and at the same time is in a field too weak for a C_β nucleus in a metallacyclobutane.[31−34] This is readily explained by competing shielding and deshielding contributions, as C_β shows both characteristics. The C_α and C_γ nuclei, which have only a deshielding contribution of the directly bonded zirconocene, appear in the expected range. The upfield shift of the Zr−H resonance indicates that it occupies a bridging position, while the number and multiplicity of the rest of the signals show that **9** is a symmetric dimer (Figure 7b). Finally, the sharp and well-resolved resonances of **9** allow for

(31) Seetz, J. W. F. L.; Heisteeg, B. J. J. V. d.; Schat, G.; Akkerman, O. S.; Bickelhaupt, F. *J. Mol. Catal.* **1985**, *28*, 71−83.
(32) Feldman, J.; Schrock, R. R. *Prog. Inorg. Chem.* **1991**, *39*, 35−42.
(33) Straus, D. A.; Grubbs, R. H. *J. Mol. Catal.* **1985**, *28*, 9−25.
(34) Gilliom, L. R.; Grubbs, R. H. *Organometallics* **1986**, *5*, 721−724.

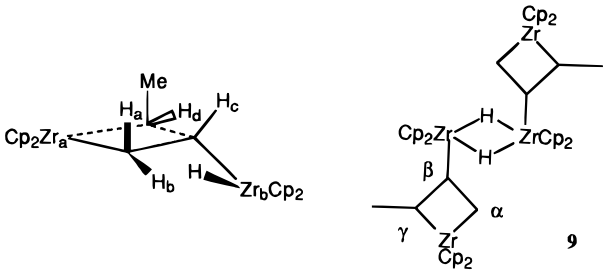

Figure 7. (a, left) Schematic representation of a fragment of the 3D structure of **9** as determined by NOESY. (b, right) Proposed structure for **9**.

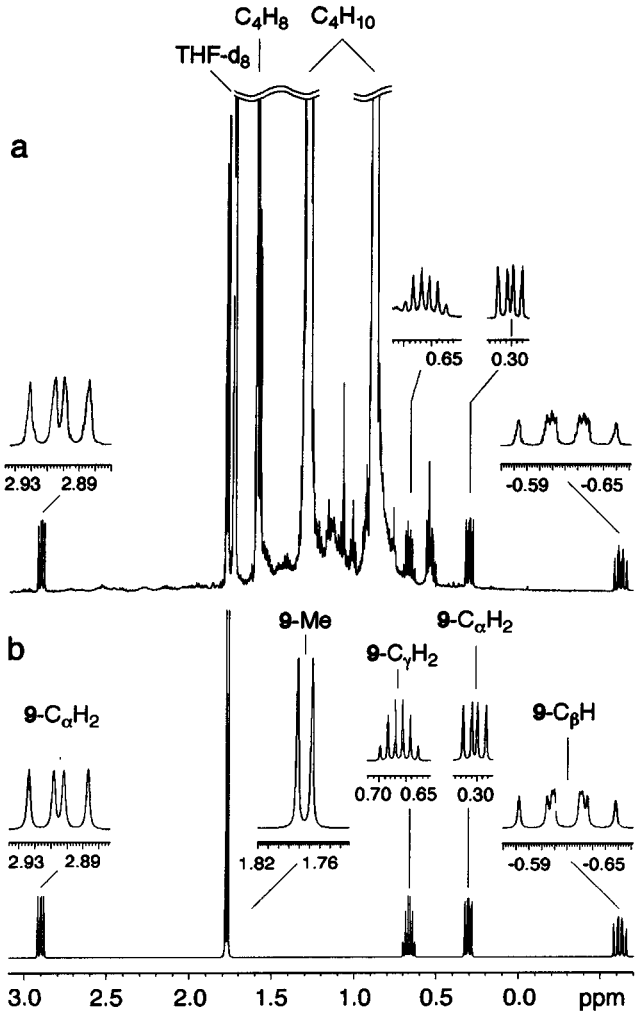

Figure 8. (a) ^{1}H NMR spectrum of **9** in THF-d_8 at +25 °C. (b) Spin simulation of the ^{1}H NMR spectrum of **9**.

determination of all coupling constants. An excellent fit between the experimental and simulated spectra (parts a and b, respectively, of Figure 8 lends further support to the assignments.

The concentration of **9** gradually increases, and it eventually becomes one of the dominant diamagnetic products in the mixture due to its high thermal stability, although its concentration never exceeds 20% of the initial concentration of **1**. A variety of uncharacterized diamagnetic products are also formed in very minor amounts. Although most of the material remains in solution, the total intensity of all the NMR signals (except butane) decreases at least by a factor of 2, relative to the solvent resonances, in the course of 0.5−1 h at room temperature. Thermal decomposition of **1** is accompanied by a change in color from yellow to black,

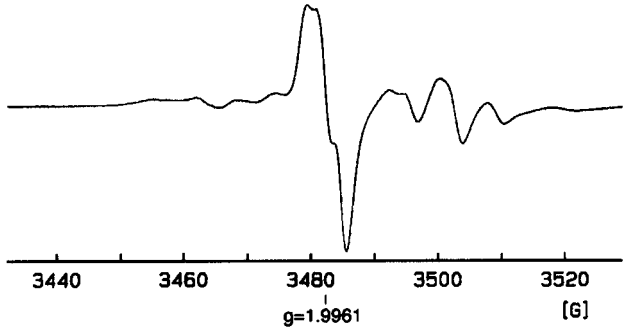

Figure 9. EPR spectrum of a mixture of **11** and unidentified paramagnetic compounds in toluene. The main peak is an apparent triplet due to the hyperfine coupling to the butyl ligand.

which is usually an indication of the formation of low-oxidation-state, paramagnetic Zr^{III} compounds. Indeed, EPR measurements (Figure 9) reveal formation of the paramagnetic species **11**, which gives an apparent triplet in toluene, due to the hyperfine coupling of the unpaired electron to two protons (g = 1.9961, a(H) = 2.4 G). The spectrum is complicated by the presence of some small amounts of other paramagnetic compounds, the signals of which mask the ^{91}Zr satellites of the main signal. Although it is not possible to measure a(Zr) accurately, an upper limit of 9 G can be estimated from the spectrum. The frozen-solution EPR spectrum is inconclusive due to the overlap of the main signal with the signals of other compounds. It is worth mentioning that no zero-field splitting has been observed.

When the paramagnetic reaction mixture is quenched with dry HCl (or with DCl in D_2O), $C_3H_7CH_3$ (or C_3H_7-CH_2D) is the only volatile product produced, except for traces of butane and butene isomers (less than 1% each). The main NMR detectable zirconium product (>99%) is Cp_2ZrCl_2. By NMR integration of the proton spectra, the Cp to C_4H_9D proton ratio is 10:8 (±1). No deuterium labels were detected in the Cp_2ZrCl_2, and no $CpZrCl_3$ was formed. Because it is known that excess BuLi leads to loss of a Cp group,[35] care was taken to ensure that there was no excess lithium reagent in the mixture prior to quenching. These observations are crucial, as a number of decomposition−reduction reactions have been previously reported, including abstraction of a Cp proton[36] and the loss of one Cp ligand from the sandwich,[37] which cannot be discriminated by EPR in the case of **11** due to the poor resolution, but can be ruled out on the basis of the NMR results. Possible candidates for the observed EPR spectra are Cp_2ZrBu, $[Cp_2ZrBu]_2$, $[Cp_2ZrBu_2]^{\bullet-}$, or $[Cp_2ZrBu{\cdot}Cp_2ZrR_2]$, where Cp_2ZrR_2 could be any diamagnetic zirconocene. The dimer $[Cp_2ZrBu]_2$ might be either diamagnetic or antiferromagnetic,[38] but the latter is inconsistent with the EPR features of **11**. The diamagnetic dimer $[Cp_2ZrBu]_2$, on the other hand, although it is not observable by EPR, could give the observed broad and featureless NMR spectrum if it is in equilibrium with a paramagnetic monomer. The amount of Zr^{III} directly measured by EPR accounts for about 5% of the total amount of Zr.

(35) Kondakov, D.; Negishi, E. *J. Chem. Soc., Chem. Commun.* **1996**, 963−964.
(36) Klei, E.; Teuben, J. H. *J. Organomet. Chem.* **1980**, *188*, 97−107.
(37) Van der Weij, F. W.; Scholtens, H.; Teuben, J. H. *J. Organomet. Chem.* **1977**, *127*, 299−304.
(38) Xin, S.; Harrod, J. F.; Samuel, E. *J. Am. Chem. Soc.* **1994**, *116*, 11562−11563.

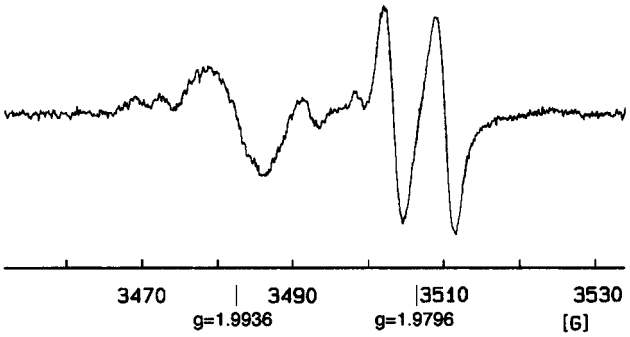

Figure 10. EPR spectrum of a mixture of **12** and $Cp_2Zr(CH_2CH{=}CHMe)$[50] in THF. The doublet peak is due to the hyperfine coupling to the hydride ligand.

The radical anion $[Cp_2ZrBu_2]^{\bullet-}$, can be ruled out as the EPR-observable species because such electron-rich compounds exhibit much higher a(Zr) and a(H) values than **11** does.[39−41] Low values for the hyperfine coupling constants, such as those presently observed, are usually attributed either to electron-withdrawing substituents[42] or electron delocalization between two metal centers,[43−45] such as in the Zr^{III}/Zr^{IV} dimer $[Cp_2ZrBu{\cdot}Cp_2ZrR_2]$. The EPR multiplicity for $[Cp_2ZrBu{\cdot}Cp_2ZrR_2]$ should be more complicated than a triplet, but with the given resolution and line width such a possibility cannot be discarded. We thus conclude that **11** is most probably the diamagnetic dimer $[Cp_2ZrBu]_2$ in equilibrium with its paramagnetic monomer or with the paramagnetic dimer $[Cp_2ZrBu{\cdot}Cp_2ZrR_2]$. The g value and the hyperfine constants are in the normal range reported for alkylzirconocenes and titanocenes.[36,41,46,47] Addition of PMe_3 does not improve the resolution and leads to a simple doubling of the EPR resonances ($Cp_2ZrBu(PMe_3)$: g = 1.9955, a(P) = 20.6 G, a(Zr) = 16.25 G, a(H) < 2 G in toluene).

The other paramagnetic products (Figure 10) are Cp_2ZrH[42,48,49] (**12**) (g = 1.9796, doublet, a(H) = 7.0 G in THF) and $Cp_2Zr(CH_2CH{=}CHMe)$[50] (broad unresolved multiplet, g = 1.9936 in THF). When toluene is used as a solvent, a more complicated multiplet is observed. Addition of PMe_3 doubles the number of resonances and results in a complicated and intractable spectrum.

It is worth mentioning that no hydrogen has been detected among the spontaneous decomposition products of **1**. By far the major hydrocarbon product is butane, accompanied by a small amount of *cis*- and *trans*-2-butene (10−15%), which are formed at the late decomposition stages and are identified by NMR.[51−53] Although 1-butene[53,54] can be detected among the hydrolysis products after HCl or DCl workup, it is not formed when the sample is kept under rigorously anaerobic conditions.

Discussion

I. Reaction Scheme for Decomposition of Cp_2ZrBu_2. The first observable product formed by decomposition of **1** is **3a**. This compound is most unlikely to be a prime decomposition intermediate, since it is hard to imagine any synchronous process which would lead directly from **1** to **3a**. There must be another intermediate in this transformation. It is usually assumed that decomposition of **1** occurs through β-H abstraction, followed by elimination of butane and formation of **2a**.[1] However, the present results show that **2a** itself is formed from **3a**. This particular order can be observed not only in the thermal decomposition of **1** but also in an independent synthesis of **3a**, where a fast rearrangement to **2a** occurs. Therefore, it is highly unlikely that **2a** can be the prime product of decomposition of **1**.

The conclusion that the primary decomposition of Cp_2ZrBu_2 probably occurs by γ- rather than β-H abstraction runs counter to previous opinion. It has been convincingly shown by experiment that β-H abstraction is preferred in the case of $Cp_2Zr(R)Et$ compounds.[55] However, it is likely that the energy difference between α-, β-, and γ-H abstraction is quite small. This is supported by a number of theoretical analyses of agostic intermediates carried out on Ziegler−Natta type systems. Indeed, some of these calculations show that the γ-agostic interaction has the lowest energy.[56−59] Inspection of molecular models of Cp_2ZrBu_2 shows that β-H abstraction requires a transition state with two flat zirconacyles lying in the same plane, and with very little conformational freedom (Figure 11a). On the other hand, γ-H abstraction, while still requiring a bicyclic transition state, leaves one ring nonplanar, with the conformational flexibility to absorb steric strain (Figure 11b). Thus, it is not unlikely that the change from an ethyl ligand to a more sterically demanding butyl ligand could tilt the reaction pathway in favor of γ-H abstraction.

The chain of transformations (**1** → ... → **3a** → **2a**) together with the product **9** (Scheme 1), derived from the postulated zirconacyclobutane, suggests that **6a** does exist in this mixture, although its concentration and

(39) Samuel, E.; Guery, D.; Vebel, J.; Basile, F. *Organometallics* **1985**, *4*, 1073−1077.
(40) Fakhr, A.; Mugnier, Y.; Gautheron, B.; Laviron, E. *Nouv. J. Chim.* **1986**, *10*, 601−605.
(41) Cardin, D. J.; Lappert, M. F.; Raston, C. L. *Chemistry of Organozirconium and -hafnium Compounds*; Ellis Horwood: Chichester, U.K., 1986.
(42) Samuel, E. *Inorg. Chem.* **1983**, *22*, 2967−2970.
(43) Samuel, E.; Harrod, J. F. *J. Am. Chem. Soc.* **1984**, *106*, 1859−1860.
(44) Gauvin, F.; Britten, J.; Samuel, E.; Harrod, J. F. *J. Am. Chem. Soc.* **1992**, *114*, 1489−1491.
(45) Bazhenova, T. A.; Kulikov, A. V.; Shestakov, A. F.; Shilov, A. E.; Antipin, M. Y.; Lyssenko, K. A.; Struchkov, Y. T.; Makhaev, V. D. *J. Am. Chem. Soc.* **1995**, *117*, 12176−12180.
(46) Klei, E.; Telgen, J. H.; Teuben, J. H. *J. Organomet. Chem.* **1981**, *209*, 297−307.
(47) Williams, G. M.; Schwartz, J. *J. Am. Chem. Soc.* **1982**, *104*, 1122−1124.
(48) Bajgur, C. S.; Jones, S. B.; Petersen, J. L. *Organometallics* **1985**, *4*, 1929−1936.
(49) Wolf, J. M. d. W.; Meetsma, A.; Teuben, J. H. *Organometallics* **1995**, *14*, 5466−5468.
(50) Under slightly different experimental conditions a well-resolved EPR spectrum of $Cp_2Zr(CH_2CH{=}CHMe)$ can be observed in these reaction mixtures: Soleil, F.; Choukroun, R.; Frances, J. M. *J. Am. Chem. Soc.*, in press.
(51) Pople, J. A.; Schneider, W. G.; Bernstein, J. H. *High Resolution Nuclear Magnetic Resonance*; McGraw-Hill: New York, 1959; p 236−238.
(52) Rummens, F. H. A.; Kaslander, L. *Can. J. Spectroc.* **1972**, *17*, 99−102.
(53) Breitmaier, E.; Voelter, W. *Carbon-13 NMR Spectroscopy: High Resolution Methods and Applications in Organic Chemistry and Biochemistry*, 3rd ed.; VCH: New York, 1987.
(54) Bothner-By, A. A.; Naar-Colin, C. *J. Am. Chem. Soc.* **1961**, *83*, 231−236.
(55) Negishi, E.; Nguyen, T.; Maye, J. P.; Choueiri, D.; Suzuki, N.; Takahashi, T. *Chem. Lett.* **1992**, 2367−2370.
(56) Meier, R. J.; van Doremaele, G. H. J.; Iarlori, S.; Buda, F. *J. Am. Chem. Soc.* **1994**, *116*, 7274−7281.
(57) Woo, T. K.; Ziegler, T. *Organometallics* **1994**, *13*, 2252−2261.
(58) Fan, L.; Harrison, D.; Woo, T. K.; Ziegler, T. *Organometallics* **1995**, *14*, 2018−2026.
(59) Margl, P.; Lohrenz, J. C. W.; Ziegler, T.; Blochl, P. E. *J. Am. Chem. Soc.* **1996**, *118*, 4434−4441.

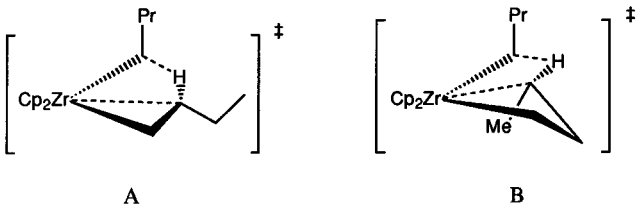

A B

Figure 11. (A) Generic σ-bond metathesis transition state for β-H abstraction. Two flat zirconacycles are lying in the same plane and have no conformational freedom. (B) Generic σ-bond metathesis transition state for γ-H abstraction. The species is still bicyclic, but one of the cycles does not have to be planar and can twist to meet the geometry requirements of the other one.

stability are insufficient for a firm identification. This is not surprising, as the reaction mixture exhibits a complicated and heavily overlapped NMR spectrum, which only allows identification of the most abundant compounds. An alternative decomposition of **1** with the prime formation of the elusive "Cp_2Zr", accompanied by reductive elimination of octane, can be ruled out at this stage since octane was not detected in the system.

Further decomposition of the postulated **6a** can proceed by β-H abstraction from either the methyl or the methylene group (Scheme 1). The former process is a reverse reaction to an olefin insertion into a Zr−H bond, where an olefin is already positioned in the coordination sphere of Zr by a flexible two-carbon-atom bridge. It is unlikely for such a β-H abstraction to be thermodynamically or kinetically favorable over the reverse insertion reaction. The β-H abstraction from the methylene group is a similar process except that the bridge is more rigid, which makes the reverse insertion reaction less favorable and the product, **3a**, more stable. Such allyl and metallacyclobutane interconversions are known; e.g. migration of hydrocarbyl fragments from a central metal to a β-position of an allyl ligand with formation of zirconacyclobutane has been reported before by Stryker *et al.* and is believed to occur via a radical process.[18,19] A concerted σ-bond metathesis process is a less likely alternative due to an unfavorable geometry of the transition state.[18,19] Such a rearrangement strongly depends on the nature of the migrating group (*e.g.* methyl in methylallylzirconocene does not migrate, whereas allyl in diallylzirconocene does)[19] and might proceed in a reverse direction in the case of a hydride, as has been reported for the late transition metals.[60]

Finally, **3a** undergoes a slow (at −40 °C) 1,3-H shift to form **5a** or an insertion of the olefin (crotyl) into the Zr−H bond to form **2a**, which is the second major observable product in the early stages of decomposition. Similar intramolecular hydrogen migrations, which interconvert metallacyclobutanes, metallacyclopropanes, and alkenyl- and allylmetal hydrides have been previously reported for early and late transition metals in relation to the catalytic isomerization of olefins.[25,60,61] A rearrangement between Cp* analogs of **2a** and **3a** has been previously cited as a possible mechanism for isomerization of alkenylzirconocene hydrides, albeit the authors have favored another pathway.[25] These processes are most likely reversible, although the equilibria are shifted almost entirely toward **2a**. Even though **3a** disappears rapidly, the products in the later stages of decomposition (**9**, **5a**, **11**, 2-butene, and butane) are more likely to be derivatives of either **6a** or **3a** and cannot be formed directly from **2a** (e.g., reductive elimination from **2a** should lead to 1-butene, which has not been detected in the absence of hydrolysis)

Although both $Cp^*_2Zr(CH_2CH{=}CHCH_3)H$, in the presence of 1- or 2-butene,[25] and $Cp^*_2ZrBu_2$[29] have been reported to produce the Cp* analog of **4a**, a mechanism for the transformation of **2a** or **3a** into **4a** is not immediately clear. Such reactions are usually explained by a simplified approach (eq 4),[1] where two olefins first

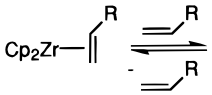

2a R=Et
2b R=Me

(4)

4a R=Et
4b R=Me

coordinate to the same d^2 Zr center and then couple together.[1] Given the fact that 1-butene was not detected in the reaction mixture, we conclude that the mechanism for this process is yet to be defined. However, the simplistic model is still useful for visualization of the reaction pathway and predictions of regio- and stereospecificity.[1] This reaction is reversible,[25] and although **4a** is a major kinetic product, it gradually rearranges back to **3a** as the latter slowly but irreversibly participates in other reactions, leading to reductive elimination (Scheme 1).

Since the most abundant hydrocarbon product is butane, the major reductive elimination must occur from zirconium center(s) bearing both butyl and hydride ligands. Such a compound, $Cp_2Zr(H)Bu$ (**7**), can be formed from **3a** by ligand redistribution with butylzirconocene. The postulated **7** has not been observed spectroscopically, which is most likely due to its extreme instability. It can either spontaneously lose butane or form a Zr−H−Zr bridged structure with other zirconocenes. When **1** is still abundant in the reaction mixture, the newly formed bridge would contain H and Bu fragments in close proximity. A dimer of **3a** and **1** is also a candidate for elimination of BuH. Such compounds are likely to undergo reductive elimination of butane with formation of **11** (Scheme 1) and $Cp_2Zr(CH_2CH{=}CHMe)$, respectively. Indeed, alkylzirconocene hydrides are known to participate in reductive-elimination reactions. The exact mechanism of such eliminations is unknown. It has been postulated to be a unimolecular, two-electron process, but experimental observations are further complicated by ligand scrambling and cyclopentadienyl C−H activation processes.[62−64] The latter do not occur in the present case, as has been shown by the DCl quenching experiment (*vide supra*).

Reductive elimination could occur from a monomeric alkylzirconocene hydride with formation of "Cp_2Zr^{II}", as

(60) Tulip, T. H.; Ibers, J. A. *J. Am. Chem. Soc.* **1979**, *101*, 4201−4211.
(61) Ohff, A.; Burlakov, V. V.; Rosenthal, U. *J. Mol. Catal., A: Chem.* **1996**, *105*, 103−110.
(62) McAlister, D. R.; Erwin, D. K.; Bercaw, J. E. *J. Am. Chem. Soc.* **1978**, *100*, 5966−5968.
(63) Wielstra, Y.; Gambarotta, S.; Meetsma, A.; Spek, A. L. *Organometallics* **1989**, *8*, 2948−2952.
(64) Miller, F. D.; Sanner, R. D. *Organometallics* **1988**, *7*, 818−825.

Scheme 1. Proposed Sequence of Reactions Occurring during Decomposition of Cp_2ZrBu_2

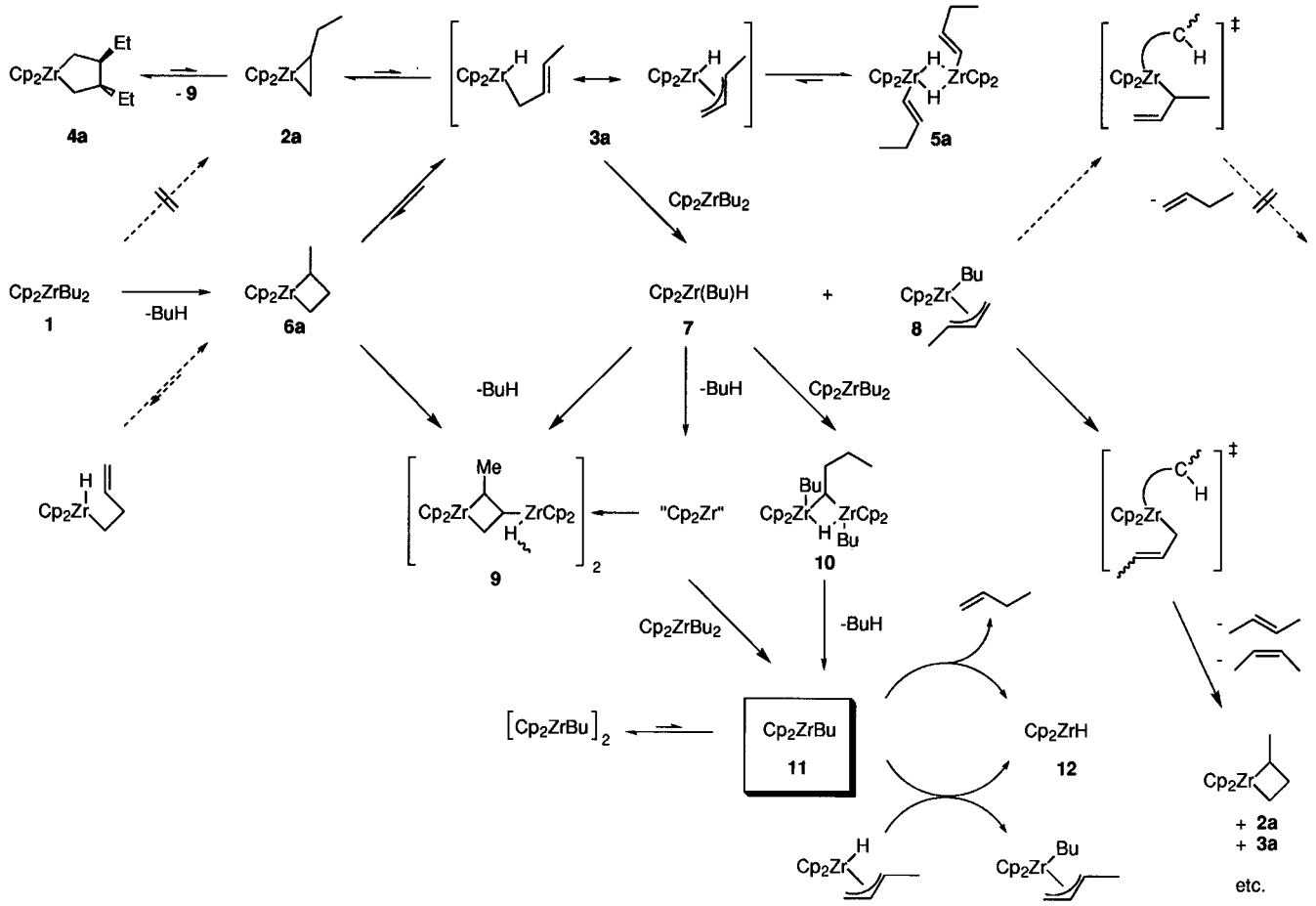

previously postulated.[65] The "Cp_2Zr^{II}" can undergo further redox conproportionation with Cp_2ZrBu_2 to form Cp_2ZrBu (Scheme 1), as has been reported before for $Cp_2Zr^{II}(PMe_3)_2$/$Cp_2Zr^{IV}X_2$.[66,67] Butylzirconocene(III) is further converted to zirconocene hydride **12** either by H elimination or ligand exchange with other hydride species. The latter is more plausible, as H elimination would most likely produce 1-butene, which has not been found. The other elimination products, *cis*- and *trans*-2-butene, can be accounted for by a similar reductive elimination from **3a** (or its dimer) or a nonreductive H abstraction from the butyl ligand in Cp_2Zr(crotyl)Bu (Scheme 1). Such a reduction of mono- and bis(cyclopentadienyl) compounds of titanium and zirconium by the MR_n alkylating agents (M = Li,[68] MgBr,[69] Al[70−72]) is a well-known, yet poorly understood reaction. It is often discussed in the context of the Ziegler−Natta polymerization reaction, as it is believed to be of relevance to the catalyst deactivation, whereas nonreductive hydrogen or alkyl eliminations are responsible for chain transfer reactions.[73,74]

The most thermally stable diamagnetic compound in this mixture and the second most abundant product, **9**, can be formed from **6a** either by insertion of "Cp_2Zr" or by a σ-bond metathesis with **7**. The presence of a zirconacyclobutyl skeleton in **9** lends further support for the existence of its precursor, **6a**, in this mixture.

II. Thermochemical Aspects of the Proposed Reaction Steps. The observed elimination products and proposed reaction pathways can be rationalized on the basis of the previously reported Zr−H and Zr−C bond disruption enthalpies of similar zirconocenes.[29,75,76] As has been reported before[29] and can be seen from the data in Table 2, modest steric effects do not have any significant influence on the BDE values (e.g. Cp_2ZrMe_2, $Cp^*_2ZrMe_2$, and $Cp_2^*Zr(\eta^1{:}\eta^1\text{-}CH_2CH_2\text{-}o\text{-}C_6H_4)$). This allows the use of the BDEs measured for Zr−alkyl bonds in $Cp_2^*Zr(\eta^1{:}\eta^1\text{-}CH_2CH_2\text{-}o\text{-}C_6H_4)$, $Cp_2Zr(n\text{-}C_6H_{13})Cl$, and $Cp_2Zr(\text{cyclo-}C_6H_{13})Cl$ as good approximations for all nonstrained Zr−(sp^3-C) bonds, with the proviso that the values for the last two compounds should be corrected for the effect of chloride ligand. The mean values reported for compounds Cp_2ZrR_2 with two identical substituents, which have been titrated in a double-stage procedure (e.g. $Cp_2ZrR_2 + 2R'OH \rightarrow Cp_2Zr(OR')R + RH + R'OH \rightarrow Cp_2Zr(OR')_2 + 2RH$), also need to be corrected to account for the effect of the electron-withdraw-

(65) Alt, H.; Rausch, M. D. *J. Am. Chem. Soc.* **1974**, *96*, 5936−5937.
(66) Gambarotta, S.; Chiang, M. Y. *Organometallics* **1987**, *6*, 897−899.
(67) Wielstra, Y.; Gambarotta, S.; Meetsma, A.; de Boer, J. L. *Organometallics* **1989**, *8*, 250−251.
(68) You, Y.; Wilson, S. R.; Girolami, G. S. *Organometallics* **1994**, *13*, 4655−4657.
(69) Martin, H. A.; Jellinek, F. *J. Organomet. Chem.* **1968**, *12*, 149−161.
(70) Bueschges, U.; Chien, J. C. W. *J. Polym. Sci., Polym. Chem. Ed.* **1989**, *27*, 1525−1538.
(71) Chien, J. C. W.; Salajka, Z.; Dong, S. *Macromolecules* **1992**, *25*, 3199−3203.
(72) Cam, D.; Sartori, F.; Maldotti, A. *Macromol. Chem. Phys.* **1994**, *195*, 2817−2826.
(73) Chien, J. C. W.; Wang, B.-P. *J. Polym. Sci., Polym. Chem. Ed.* **1990**, *28*, 15−38.
(74) Huang, J.; Rempel, G. L. *Prog. Polym. Sci.* **1995**, *20*, 459−526.
(75) Christ, C. S.; Eyler, J. R.; Richardson, D. E. *J. Am. Chem. Soc.* **1990**, *112*, 4778−4787.
(76) Diogo, H. P.; de Alencar Simoni, J.; Minas de Piedade, M. E.; Dias, A. R.; Martinho-Simoes, J. A. *J. Am. Chem. Soc.* **1993**, *115*, 2764−2774.

Table 2. Bond Disruption Enthalpies (kcal/mol)

bond (compd)	D	D_{cor}	ref
Zr−Me (Cp_2ZrMe_2)	67	62.5[a]	76
Zr−Me ($Cp^*_2ZrMe_2$)	67	62.5[a]	29
Zr−H ($Cp^*_2ZrH_2$)			
first stage	75[b]	75	29
second stage	84		
Zr−H ($Cp_2Zr(Cl)H$)	87	75[c]	76
Zr−(sp^3-C) ($Cp_2Zr(Cl)$-*n*-C_6H_{13})	76	64[c]	76
Zr−(sp^3-C) ($Cp_2Zr(Cl)$-cyclo-C_6H_{11})	76	64[c]	76
Zr−(sp^3-C) ($Cp_2*Zr(\eta^1{:}\eta^1$-CH_2CH_2-*o*-$C_6H_4)$)	63.1	63.1	
strained Zr−(sp^3-C) ($Cp_2*Zr(\eta^1{:}\eta^1$-$CH_2CH(Et)CH(Et)CH_2)$)	53.5	49[a]	29
strained Zr−(sp^3-C) ($Cp*Zr(Ph)(\eta^1{:}\eta^5$-$C_5Me_4CH_2)$)	45	45[d]	29
Zr−(sp^2-C) ($Cp^*_2ZrPh_2$)	73	73[d]	29
Zr−allyl ($Cp_2Zr(allyl)^+$), minimal value		$D_{Zr-alkyl} + 15$	75
(sp^3-C)−H (H-CH_2CH_3)	98	98	82
allylic C−H (H-$CH_2CH{=}CH_2$)	85	85	82
(sp^2-C)−H (H-$CH{=}CH_2$)	103	103	82
C-C (CH_3-CH_2CH_3)	85	85	82
π component of C=C ($CH_2{=}CH_2$)	75	75	82
H−H (H_2)	104	104	82

[a] The mean values, reported for compounds Cp_2ZrX_2 with two identical substituents, which had been titrated in a double-stage procedure (e.g. $Cp_2ZrMe_2 + ROH \rightarrow Cp_2Zr(OR)Me + MeH \rightarrow Cp_2Zr(OR)_2 + MeH$), were corrected to account for the effect of the electron-withdrawing substituent (OR) on the BDE in the second stage. The correction coefficient was estimated from the BDEs of Zr−H bonds in Cp_2ZrH_2, for which the separate stage and the mean BDEs are both available, and was assumed to be approximately the same for all Cp_2ZrX_2 compounds. [b] Two titration stages had been done separately and do not need any correction. [c] The values, reported for $Cp_2Zr(Cl)X$, were corrected for the effect of the electron-withdrawing ligand (Cl). A correction coefficient was estimated from the difference in the BDEs of Zr−H bonds in Cp_2ZrH_2 and $Cp_2Zr(Cl)H$ and was assumed to be approximately the same for all $Cp_2Zr(Cl)X$ compounds. [d] Only the first titration stage was performed, and the value does not require any correction.

ing substituent (OR′) on the BDE in the second stage. Such a correction can be done by assuming $D_{[ZrH]-alkyl} - D_{[ZrH]-H} = D_{[ZrX]-alkyl} - D_{[ZrX]-H}$, which is derived from a modified version of the bond enthalpy equation of Matcha as suggested by Schock and Marks.[29] A correction coefficient has been calculated from the BDEs of Zr−H bonds in Cp_2ZrH_2, for which the separate stage and the mean BDEs are both available, and is assumed to be approximately the same for all Cp_2ZrR_2 compounds. All BDEs for the nonstrained Zr−alkyl bonds, reported for similar compounds by different authors, exhibit an excellent agreement after correction. Furthermore, a steric strain in the zirconacarbocycles can also be estimated. Thus, $Cp_2*Zr(\eta^1{:}\eta^1$-$CH_2CH(Et)CH(Et)CH_2)$ and $Cp*Zr(\eta^1{:}\eta^5$-$C_5Me_4CH_2)$ can be used as examples of strained molecules and their Zr−alkyl BDEs are 7.5 (per Et group) to 19 kcal/mol smaller, reflecting the steric strain. The latter compound can be viewed as an extremely strained cycle, and it sets an upper limit for the ring strain energy. The former complex gives a more realistic 7−8 kcal/mol steric strain, arising from nonbonding repulsion of the Et groups and Cp* rings, whereas the ring strain itself in the four-membered and larger zirconacarbocycles is fairly small (e.g. a Zr−alkyl BDE in $Cp_2*Zr(\eta^1{:}\eta^1$-CH_2-CH_2-*o*-$C_6H_4)$ is indistinguishable from the values for any nonstrained Zr−alkyl bond as the hydrocarbyl fragment is flat and has neither ring strain nor any significant nonbonding interactions with the Cp* ligands). In the case of unsubstituted Cp the nonbonding repulsion should be even smaller.

With no accurate experimental data available for zirconacyclopropane and zirconacyclobutane compounds, we have chosen arbitrary steric strain values of 15 and 8 kcal/mol per cycle, respectively. Thus, the calculated reaction enthalpies should be treated only as rough estimates because the starting BDE values are of limited accuracy. ΔG_{calcd} can be estimated by assuming that the $T\Delta S$ contribution of creating an additional particle near room temperature is ca. -9 ± 3 kcal/mol,[29] which adds further uncertainty to our calculations. With all the limitations taken into consideration, this approach can still provide valuable information, as most of the reactions in question are estimated to be very endothermic by more than 30 kcal/mol (eqs 6, 7, 9, and 10) and are unlikely to occur even if there are large errors in the starting BDEs. Calculating interconversions of zirconacyclobutanes, zirconacyclopropanes, and alkenyl- and allylmetal hydrides, on the other hand, would be meaningless, as the margin of error for them is higher than the expected effect itself.

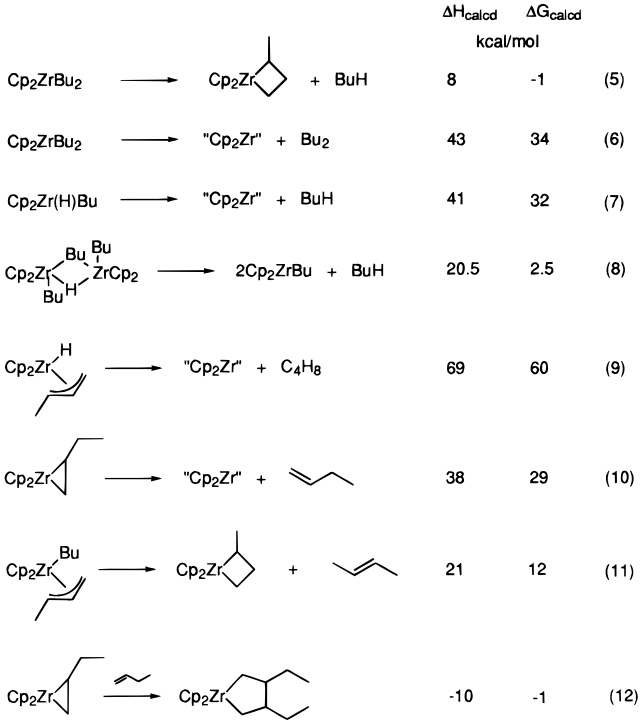

As can be seen from the results of our calculation, the three most favorable elimination processes account for the formation of the major identified or postulated compounds: **6a** (or isomers **2a** and **3a**; eq 5), **4a** (eq 12),

11 and butane (eq 8). The only thermodynamically feasible reductive elimination is the elimination from the dimeric [Zr(μ-H)(μ-Bu)Zr] (**10**) and is due to an entropy gain. Alternative reductive eliminations from monomeric [Zr(H)R] (**7**, and **3a**) or from **2a** are highly endothermic (eqs 7, 9, and 10). In the case of R = crotyl, which is a bulky four-electron-donor ligand, formation of a dimer is unlikely to occur, which makes reductive elimination unfavorable and explains the absence of 1-butene among the products. 2-Butene, on the other hand, can be formed via a thermodynamically more favorable nonreductive route (eq 11 and Scheme 1). The transition state for the same H-abstraction, which would lead to 1-butene, is considerably more constrained (Scheme 1); hence, 1-butene is not formed. An absence of any observable quantities of dihydrogen or octane among the products is in good agreement with the observed intermediates, proposed decomposition pathway, and thermochemical calculations (eq 6).

When the starting compounds are zirconocene chloride hydride and crotylmagnesium bromide, the scrambling−dimerization−reductive-elimination sequence is not the major reaction pathway, as no hydrocarbyl ligands other than crotyl are available and it is too coordinatively demanding to allow any significant dimerization (e.g. to form the crotyl analog of **10**) (*vide supra*). With dimerization being unfavorable, the equilibrium shifts toward the zirconacyclopentane **4a** and zirconacyclobutane **9**, which are kinetically stable for days at room temperature. Reduction of zirconium(IV) does not occur.

Conclusions

Cp_2ZrBu_2 is unstable with respect to elimination of butane by γ-hydrogen abstraction from the neighboring butyl group, leading to the zirconacyclobutane **6a**. The latter has not been detected directly but is postulated on the basis of the observed product **9** and other reactions in the system. **6a** rearranges to form crotylzirconocene hydride **3a**, which undergoes further rearrangement to produce the zirconacyclopropane **2a** and the dimeric butenylzirconocene hydride **5a**. In the early stages of decomposition the most abundant diamagnetic products are **2a** and **3a**. Further thermolysis leads to the formation of **4a**, **5a**, and **9**. Compounds **4a**, **5a**, and **9** are stable for days at room temperature, but the first two are in equilibrium with **3a**. When the starting material is Cp_2ZrBu_2, unconsumed Cp_2ZrBu_2 reacts with **3a** by ligand exchange or dimerization and reductive elimination occurs to produce zirconocene with zirconium in oxidation state III. Compounds **4a** and **5a** are consumed accordingly, to eventually give Cp_2ZrR (R = Bu, crotyl, H) and other minor paramagnetic compounds**.** If **3a** is synthesized directly from zirconocene chloride hydride and crotylmagnesium bromide (in the absence of Cp_2ZrBu_2), the ligand exchange−dimerization−reductive-elimination sequence is not the major reaction pathway, as no hydrocarbyl ligands other than crotyl are available and it is too coordinatively demanding to allow any significant dimerization (e.g. to form the crotyl analog of **10**). With dimerization being unfavorable, the equilibrium shifts toward the zirconacyclopentane **4a**, which is kinetically stable for days at room temperature, and reduction of zirconium does not occur. The thermal instability of many of the key zirconocene intermediates and the suppression of the reduction pathway by unsaturated ligand (e.g. crotyl) provide an explanation for the necessity of adding the unsaturated reactant in Negishi cyclometalations before the mixture is brought to room temperature.[1]

Although it has not been possible to identify all of the decomposition products, the very fact that the Cp_2ZrCl_2/2BuLi reagent contains substantial amounts of Zr^{III} is very important. It explains the reactivity origins of the Cp_2ZrCl_2/2BuLi reagent in the dehydropolymerization of silanes[13,14,77−79] and sheds new light on the reaction mechanism.[14]

Experimental Section

Materials and Methods. All operations were performed in Schlenk-type glassware on a dual-manifold Schlenk line or in an argon-filled M. Braun Labmaster 130 glovebox (<0.05 ppm of H_2O). Argon was purchased from Matheson (prepurified for the glovebox and UHP for the vacuum line) and was used as received. The solvents (protio- and deuteriobenzene, toluene, and THF) were dried and stored over Na/K alloy, benzophenone, and 18-crown-6 in Teflon-valved bulbs and were vacuum-transferred prior to use. Crotyl bromide and $CDCl_3$ were stored over molecular sieves. Cp_2ZrCl_2, $[Cp_2Zr(H)Cl]_2$, *n*-BuLi (1.6 M in C_6H_{14}), Mg turnings, $MeCH{=}CHCH_2Br$, $CH_2{=}CHCH_2MgBr$ (1.0M in Et_2O), C_6D_6, C_7D_8, C_4D_8O, and $CDCl_3$ were purchased from Aldrich and used as received unless stated otherwise.

Physical and Analytical Measurements. Grignard reagents and *n*-BuLi were titrated with a solution of *sec*-BuOH in xylene, using 2,2′-biquinoline as an indicator.[80] NMR spectra were recorded on a Varian Unity 500 (FT, 500 MHz for ^1H) spectrometer. Chemical shifts for ^1H and ^{13}C spectra were referenced using internal solvent resonances and are reported relative to tetramethylsilane. EPR spectra were recorded on a Bruker ESP 300E (X-band) spectrometer and were referenced to external DPPH. All samples for spectroscopic measurements were flame-sealed in NMR tubes under vacuum. Quantitative EPR measurements were performed with an external standard of TEMPO of known concentration. A number of experiments were done with different acquisition parameters (modulation and microwave power) to ensure that there was no saturation of the signal. The other acquisition parameters were compensated for by a system normalization constant and were usually kept constant for both the unknown and the standard sample measurements.

Preparation of a Cp_2ZrBu_2 NMR Sample. A solution of *n*-BuLi in hexanes (0.10 mL, 0.25 mmol) was syringed into an NMR tube assembly, consisting of two 5 mL round-bottom flasks fitted with a Teflon valve to which an NMR tube has been fused at an angle of 45°. The solvent was removed under vacuum, and the residue was redissolved in toluene-d_8 or THF-d_8 (0.1-0.2 mL). The evaporation−vacuum transfer cycle was repeated twice to remove any residual hexanes, and a final fresh portion of toluene-d_8 or THF-d_8 (0.6-0.7 mL) was vacuum-transferred into the assembly. Cp_2ZrCl_2 (36.5 mg, 0.125 mmol) was loaded in the side bulb without coming in contact with BuLi. The apparatus was immersed in a CH_3CN−dry ice bath (−41 °C), and the reagents were mixed together and stirred for 30 min. The cold, light yellow mother liquor was decanted into the cooled NMR tube. The top part of the tube was washed by touching it with a swab of cotton wool soaked with liquid nitrogen, which causes condensation of the solvent vapors on the inner walls. The sample was then frozen, flame-sealed, and stored at −41 °C until it was loaded in the precooled (−40 °C) probe of the NMR instrument.

(77) Corey, J. Y.; Huhmann, J. L.; Zhu, X.-H. *Organometallics* **1993**, *12*, 1121−1130.
(78) Corey, J. Y.; Zhu, X.-H. *Organometallics* **1992**, *11*, 672−683.
(79) Shaltout, R. M.; Corey, J. Y. *Tetrahedron* **1995**, *51*, 4309−4320.
(80) Watson, S. C.; Eastham, J. F. *J. Organomet. Chem.* **1967**, *9*, 165.

Thermal Decomposition of Cp_2ZrBu_2. The first set of NMR measurements (1D ^1H and ^{13}C, COSY, and HMQC) was done at −40 °C. After that, the sample was warmed to +20 °C for 10 min and was then cooled down to −10 °C to prevent further decomposition. 1D ^1H NMR measurements were performed after every 10 min freeze−thaw cycle until spectral evidence for considerable changes in the sample composition was apparent. A complete set of NMR experiments (1D ^1H and ^{13}C, TOCSY, COSY, HMQC, and NOESY) was then performed. The sample was then subjected to another sequence of the freeze−thaw cycles as described above and another set of 1D and 2D NMR measurements. For each set of 2D NMR experiments the acquisition temperature was different (within the 0 through −40 °C range), whereas within a set it was constant. The variation of temperature allowed resolution of some of the cross peaks, which were otherwise overlapped. For the sample in THF-d_8 the 2D NMR experiments were done after exposing it to +20 °C for 0, 0.5, 4 and 9 h; for the sample in toluene-d_8 this occurred after 0, 0.2, 3, and 6 h.

EPR: Cp_2ZrBu (toluene, +25 °C), $g = 1.9961$ (t, $a(H) = 2.4$ G, $a(Zr) < 9$ G); Cp_2ZrBu (THF, +25 °C), $g = 1.9936$ (br m); Cp_2ZrH (THF, +25 °C), $g = 1.9796$ (d, $a(H) = 7.0$ G).

$Cp_2ZrBu(PMe_3)$. A solution of Cp_2ZrBu was prepared as follows: Cp_2ZrCl_2 (730 mg, 2.5 mmol) and a stirring bar were loaded in a Schlenk tube, and toluene (3 mL) was vacuum-transferred onto the solid. The solution was cooled to −41 °C, and *n*-BuLi (2.5 M in hexanes, 2 mL, 5.0 mmol) was added by syringe. The mixture was stirred for 1 h at −41 °C. This solution was then slowly warmed to ambient temperature, whereupon the color changed from light yellow to brown and then black. After it stood for 24 h at +25 °C, the product was treated with 1.0 M PMe_3 in toluene (5 mL, 5 mmol). EPR and NMR samples were prepared as described above. Practically no NMR signals were detected.

EPR (toluene, +25 °C): $g = 1.9955$ (d, $a(P) = 20.6$ G, $a(Zr) = 16.25$ G, $a(H) < 2$ G).

Preparation of $MeCH{=}CHCH_2MgBr$. A simplified modification of the previously reported procedure[81] was used. Magnesium turnings (187 mg, 7.7 mmol) and THF (20 mL) were loaded in a Schlenk flask. The mixture was cooled to 0 °C, and $MeCH_2{=}CHCHBr$ (0.72 mL, 7.0 mmol) was added via a syringe. An exothermic reaction occurred, and the mixture turned milky gray. It was then stirred for 24 h at room temperature, and the precipitate was allowed to settle. The clear supernatant solution was transferred to a storage flask; part of it was titrated, and the rest was used for further reactions.

Preparation of a $Cp_2Zr(RCH{=}CHCH_2)H$ (R = Me, H) NMR Sample. A solution of $(CH_2{=}CHCHR)MgBr$ in Et_2O or THF (0.20 mmol) was syringed into the NMR tube assembly described above. The solvent was removed under vacuum, a small amount of THF-d_8 (0.1−0.2 mL) was vacuum-transferred, and the sample was thawed out and stirred at 20 °C for 5−10 min. The evaporation−vacuum-transfer cycle was repeated twice to remove any residual protio solvent, and a final fresh portion of THF-d_8 (0.6-0.7 mL) was vacuum-transferred into the assembly. $[Cp_2Zr(H)Cl]_2$ (51.5 mg, 0.10 mmol) was loaded in the side bulb without coming in contact with the Grignard reagent. The apparatus was immersed in a CH_3CN−dry ice bath (−41 °C), and the reagents were mixed together and stirred for 2 h at approximately −20 °C. The cold, yellow-orange mother liquor was decanted into the cooled NMR tube, frozen, flame-sealed and stored at −196 °C until it was loaded in the precooled (−40 °C) probe of the NMR instrument. NMR experiments were performed at 0, −20, and −40 °C.

Quenching with HCl or DCl. A solution of Cp_2ZrBu_2 was prepared as follows: Cp_2ZrCl_2 (730 mg, 2.5 mmol) and a stirring bar were loaded in a Schlenk tube, and toluene (3 mL) was vacuum-transferred onto the solid. The solution was cooled to −41 °C, and *n*-BuLi in hexanes (2 mL of a 1.6 M solution) was added by syringe. The mixture was stirred for 1 h at −41 °C. This solution was then slowly warmed to ambient temperature, whereupon the color changed from light yellow to brown and then black. It was left for 24 h at +25 °C; then an aliquot of the solution was transferred into a side bulb of the NMR tube assembly, described above, and the solvent was evaporated off. Any residual solvent was removed by two evaporation−vacuum-transfer cycles with 0.2 mL portions of C_6D_6. (In the case of the DCl/D_2O reagent an additional portion of C_6D_6 was vacuum-transferred and left frozen in the NMR tube.) A solution of dry HCl gas in $CDCl_3$ (sample 1) or DCl in D_2O (sample 2) was syringed into the second side bulb of the NMR tube assembly and frozen. The assembly was put under vacuum and sealed with a Teflon valve. The acid solution was allowed to thaw out and mix with the Cp_2ZrBu_2 decomposition products.

In the case of the $HCl/CDCl_3$ reagent everything was transferred into the NMR tube and frozen; the tube was then sealed and this mixture used for quantitative NMR measurements of the ratio of Cp versus other hydrocarbon protons.

In the case of the DCl/D_2O reagent the gases and volatile liquids were condensed at −196 °C (most of the D_2O was left behind) into the NMR tube, which was then flame-sealed (sample 2). The remaining solids were dried under vacuum and dissolved in $CDCl_3$ (sample 3).

$^{13}C\{H\}$ NMR ($CDCl_3$, sample 1): δ 13.91 (s, CH_3), 25.13 (s, CH_2).

$^{13}C\{H\}$ NMR (C_6D_6, sample 2): δ 13.62 (t, $^1J_{CD} = 18.8$ Hz, CH_2D), 13.92 (s, CH_3), 25.06 (t, $^3J_{CD} = 0.4$ Hz, $CH_2CH_2CH_2D$), 25.12 (t, $^2J_{CD} = 0.8$ Hz, CH_2CH_2D).

^1H NMR ($CDCl_3$, sample 3): δ 6.37 (s, Cp_2ZrCl_2).

Acknowledgment. Financial support for this work from the NSERC of Canada and Fonds FCAR du Québec is gratefully acknowledged.

Supporting Information Available: Additional NMR spectra (12 pages). Ordering information is given on any current masthead page.

OM960543A

(81) Whitesides, G. M.; Nordlander, J. E.; Roberts, J. D. *Discuss. Faraday Soc.* **1962**, *34*, 185−190.

(82) Gordon, A. J.; Ford, R. A. *The Chemist's Companion: A Handbook of Practical Data, Techniques, and References*; Wiley: New York, 1972; pp 112−113.